

OCP: Orthogonal Constrained Projection for Sparse Scaling in Industrial Commodity Recommendation

Chen Sun
sunchen59@jd.com

Beilin Xu
xubeilin.1@jd.com

Boheng Tan
tanboheng.1@jd.com

Jiacheng Wang
wangjiacheng.52@jd.com

Yuefeng Sun
sunnyuefeng6@jd.com

Rite Bo
borite.1@jd.com

Ying He
JD.com
Beijing, China
heying.146@jd.com

Yaqiang Zang*
JD.com
Beijing, China
zangyaqiang.1@jd.com

Pinghua Gong*
JD.com
Beijing, China
gongpinghua1@jd.com

Abstract

In industrial commodity recommendation systems, the representation quality of Item-Id vocabularies directly impacts the scalability and generalization ability of recommendation models. A key challenge is that traditional Item-Id vocabularies, when subjected to sparse scaling, suffer from low-frequency information interference, which restricts their expressive power for massive item sets and leads to representation collapse. To address this issue, we propose an Orthogonal Constrained Projection method to optimize embedding representation. By enforcing orthogonality, the projection constrains the backpropagation manifold, aligning the singular value spectrum of the learned embeddings with the orthogonal basis. This alignment ensures high singular entropy, thereby preserving isotropic generalized features while suppressing spurious correlations and overfitting to rare items. Empirical results demonstrate that OCP accelerates loss convergence and enhances the model's scalability; notably, it enables consistent performance gains when scaling up dense layers. Large-scale industrial deployment on JD.com further confirms its efficacy, yielding a 12.97% increase in UCXR and an 8.9% uplift in GMV, highlighting its robust utility for scaling up both sparse vocabularies and dense architectures.

CCS Concepts

• **Information systems** → Recommender systems.

Keywords

Recommender systems, orthogonal constraint, sparse scaling

ACM Reference Format:

Chen Sun, Beilin Xu, Boheng Tan, Jiacheng Wang, Yuefeng Sun, Rite Bo, Ying He, Yaqiang Zang, and Pinghua Gong. 2018. OCP: Orthogonal Constrained

*Corresponding author.

Permission to make digital or hard copies of all or part of this work for personal or classroom use is granted without fee provided that copies are not made or distributed for profit or commercial advantage and that copies bear this notice and the full citation on the first page. Copyrights for components of this work owned by others than the author(s) must be honored. Abstracting with credit is permitted. To copy otherwise, or republish, to post on servers or to redistribute to lists, requires prior specific permission and/or a fee. Request permissions from permissions@acm.org.

Conference acronym 'XX, Woodstock, NY

© 2018 Copyright held by the owner/author(s). Publication rights licensed to ACM.

ACM ISBN 978-1-4503-XXXX-X/2018/0

<https://doi.org/XXXXXXXX.XXXXXXX>

Projection for Sparse Scaling in Industrial Commodity Recommendation . In *Proceedings of Make sure to enter the correct conference title from your rights confirmation email (Conference acronym 'XX)*. ACM, New York, NY, USA, 5 pages. <https://doi.org/XXXXXXXX.XXXXXXX>

1 Introduction

Modern industrial recommendation systems process massive and heterogeneous feature sets to model complex user behaviors. Among all input features, item representation quality is a core factor behind final performance. In practice, item features usually include categorical IDs, Item-IDs, and semantic IDs (SIDs).

Item-IDs and categorical entities are typically mapped to high-dimensional vectors through trainable lookup tables. During training, each input ID retrieves its embedding, and the embedding parameters are optimized end-to-end together with the recommendation objective. This paradigm is widely adopted in models such as YouTube DNN[3], DeepFM[4], and DIN[18]. SIDs are ordered code-words obtained by encoding item text/content into dense vectors with a pre-trained encoder and then quantizing them[1, 7, 8, 11]. They allow semantically similar items to share statistical strength, which is especially helpful for cold-start and long-tail scenarios.

To capture subtle preference signals (for example, user affinity for a specific brand-model pair), models still need fine-grained Item-ID features. This shift from coarse to fine-grained representation has pushed industrial systems into the *sparse scaling* regime[12–14], where vocabulary size V expands from millions to billions to cover long-tail inventory. However, sparse scaling introduces a major optimization issue. User-item interactions are highly skewed, so frequent items receive dense updates while most long-tail Item-IDs are rarely updated. Over time, optimization concentrates on a few dominant directions, causing effective rank degradation in embedding space, i.e., embedding collapse.

For the purpose of improving representation quality, enforced orthogonality, such as orthogonal codebook regularization and orthogonal residual quantization[5, 9, 10, 15–17], is adopted in recommendation system. Orthogonal Rotation Transformation is employed to rotate the subspace spanned by low-cardinality static features including categorical IDs[14]. Meanwhile, Item-ID remains the finest-grained identifier and has the highest cardinality in production systems. Without proper constraints, models may overfit by memorizing sparse long-tail IDs rather than learning transferable

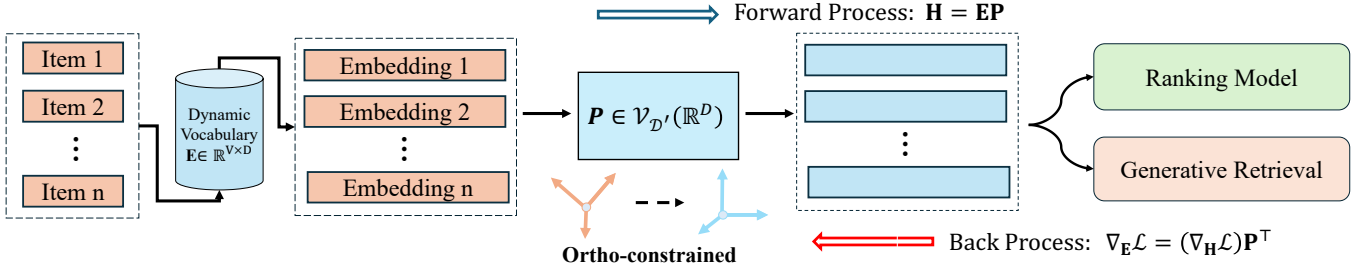


Figure 1: Overview of OCP.

patterns. To address this, we propose OCP (Orthogonal Constrained Projection) for Item-ID embedding optimization. Our contributions are:

- We characterize embedding collapse in sparse scaling and use Singular Entropy (SE) to quantify representation isotropy. The analysis explains how long-tail sparsity induces dimensional redundancy.
- We constrain the projection matrix on the Stiefel manifold[2], which preserves gradient geometry and stabilizes the singular-value distribution of embeddings.
- We validate OCP with both offline experiments and large-scale online deployment. The online model achieves +12.97% UCXR and +8.95% GMV, showing effectiveness under both sparse (vocabulary) and dense (architecture) scaling.

2 Methodology

In this section, we first formalize sparse scaling (Section 2.1), then analyze embedding collapse in sparse vocabularies (Section 2.2), and finally present OCP with its theoretical properties (Section 2.3).

2.1 Preliminary

In industrial recommendation systems, representation quality sets the performance ceiling. Category IDs provide stable global semantics with low cardinality; SIDs derived from clustering or pre-trained encoders capture intermediate-granularity semantics; Item-IDs provide the finest-grained identity with very high cardinality.

Formally, let $\mathbf{E} \in \mathbb{R}^{V \times D}$ denote the Item-ID embedding matrix and let $\mathbf{P} \in \mathbb{R}^{D \times D'}$ be a projection matrix for downstream interaction layers:

$$\mathbf{H} = \mathbf{E}\mathbf{P}. \quad (1)$$

While Sparse Scaling endows the model with the capacity to represent long-tail items, it simultaneously introduces a fundamental challenge rooted in distributional imbalance. The majority of entries in \mathbf{E} correspond to extremely low-frequency Item-IDs, which receive insufficient gradient updates due to sparse interaction data. More critically, under the conventional unconstrained parameterization of \mathbf{P} , the absence of directional constraints on gradient flow triggers a pathological phenomenon known as dimensional collapse: the effective rank of the learned representation space degrades as optimization concentrates update signals along a small subset of dominant dimensions.

2.2 Embedding Collapse in Scaled Models

Empirical evidence suggests that sparse scaling often leads to embedding collapse[5]. Despite the high-dimensional embedding space \mathbb{R}^D , the learned embedding vectors \mathbf{E} tend to reside in a much lower-dimensional manifold. This dimensionality redundancy implies that the model fails to utilize its increased capacity, resulting in stagnant or even degraded performance as the model scales.

To quantify collapse severity and information density, we use Singular Entropy (SE)[10]. For $\mathbf{E} \in \mathbb{R}^{V \times D}$ with singular values $\{\sigma_1, \sigma_2, \dots, \sigma_k\}$ ($k = \min(V, D)$), define energy $e_i = \sigma_i^2$ and normalized energy $p_i = e_i / \sum_{j=1}^k e_j$. SE is defined as:

$$\text{SE}(\mathbf{E}) = -\frac{1}{\log(k)} \sum_{i=1}^k p_i \log(p_i). \quad (2)$$

A higher SE (closer to 1) indicates a more isotropic and better-utilized embedding space; a lower SE indicates concentration in a few dominant dimensions and thus more severe collapse.

2.3 Orthogonal Constrained Projection Layer

2.3.1 Orthogonal Constraint on Stiefel Manifold. In industrial recommendation architectures, the high-cardinality Item-ID embedding matrix $\mathbf{E} \in \mathbb{R}^{V \times D}$ is mapped to an interaction space via a projection layer $\mathbf{P} \in \mathbb{R}^{D \times D'}$: $\mathbf{H} = \mathbf{E}\mathbf{P}$, where V is vocabulary size, $\mathbf{H} \in \mathbb{R}^{V \times D'}$ is the projected representation, and D is embedding dimension. Under sparse scaling, \mathbf{E} often occupies a low-dimensional subspace, i.e., $\text{rank}(\mathbf{E}) \ll \min(V, D)$.

To avoid unconstrained optimization that may further distort gradient geometry, we optimize \mathbf{P} on the Stiefel manifold:

$$\mathcal{V}_{D'}(\mathbb{R}^D) = \{\mathbf{P} \in \mathbb{R}^{D \times D'} \mid \mathbf{P}^\top \mathbf{P} = \mathbf{I}_{D'}\}.$$

We apply a projection-based update:

$$\mathbf{P} \leftarrow \text{QR}(\mathbf{P} - \eta \nabla_{\mathbf{P}} \mathcal{L}).$$

This mechanism ensures forward-backward consistency: In the forward pass, \mathbf{P} acts as an isometry, embedding high-cardinality items into a latent space without losing relative geometric relationships. In the backward pass, as derived in (3), the gradient $\nabla_{\mathbf{E}} \mathcal{L}$ inherits the singular value spectrum of the upstream task gradient, effectively forcing the model to explore a broader representation space for infrequent items by ensuring gradient’s orthogonality.

$$\nabla_{\mathbf{E}} \mathcal{L} = \frac{\partial \mathcal{L}}{\partial \mathbf{H}} \frac{\partial \mathbf{H}}{\partial \mathbf{E}} = (\nabla_{\mathbf{H}} \mathcal{L}) \mathbf{P}^\top, \quad (3)$$

where $\nabla_{\mathbf{H}}\mathcal{L} \in \mathbb{R}^{V \times D'}$ represents the upstream gradient from the interaction layers.

2.3.2 Analysis of Singular Value Preservation. Since \mathbf{P} is column-orthogonal ($\mathbf{P}^T\mathbf{P} = \mathbf{I}$), it acts as an isometry on the projected subspace. Therefore, for $i \leq \text{rank}(\nabla_{\mathbf{H}}\mathcal{L})$, the non-zero singular values are preserved during backpropagation:

$$\sigma_i(\nabla_{\mathbf{E}}\mathcal{L}) = \sigma_i((\nabla_{\mathbf{H}}\mathcal{L})\mathbf{P}^T) = \sigma_i(\nabla_{\mathbf{H}}\mathcal{L}). \quad (4)$$

This alignment ensures that the gradient flow does not suffer from further rank erosion caused by the projection weights. By preventing the "squeezing" of the gradient manifold, OCP forces the embeddings of low-frequency items to be updated along diverse orthogonal directions, effectively "stretching" the representation space and mitigating embedding collapse.

3 Experiments

3.1 Experimental Setup

We evaluate OCP on both a generative retrieval model and a ranking model in JD.com's production environment.

3.1.1 Baseline. For generative retrieval, we use OxygenREC[6] as baseline, which retrieves items using three-level SIDs. For ranking, we use an online production model from a large e-commerce scenario at JD.com as baseline for both offline and online evaluations.

3.1.2 Evaluation Metric. For OxygenREC, we report Top1 hit@k ($k = 1, 2, 3$), which measures whether the model correctly predicts the first-level SID, the first two SID levels, and the full three-level SID, respectively. For ranking, we report AUC and GAUC.

3.1.3 Training and Evaluation Protocol. For fair comparison, baseline and OCP models share the same backbone architecture, data split, optimizer family, and training budget (same number of steps). Unless otherwise specified, vocabulary settings follow each experiment configuration. For offline experiments, OCP is the only additional component over baseline. Offline metrics are computed on held-out data, and online results are reported from controlled A/B testing against the production baseline.

3.1.4 Reproducibility Notes. To improve reproducibility, we report key setup details used throughout the paper: (1) ranking experiments are trained on four months of interaction logs; (2) the SE analysis uses a $d = 64$ Item-ID embedding slice; (3) sparse scaling experiments vary vocabulary from 1e to 10e ($1e = 10^8$). The generative model was trained for 196K steps on a dataset of 6.4 billion samples, while the ranking model underwent 720K steps of training on 2.9 billion samples.

3.2 Overall Performance

Table 1 presents the overall prediction performance in our generative retrieval model. The sparse Item-ID vocabulary size is set to 0.5 billion. Compared to baseline, proposed method obtained higher Top1 hit@k ($k=1,2,3$) rate on both 0.7B and 3.2B model. After scaling up the model density, QR orthogonalization continued to yield improvements in evaluation metrics. Unlike baselines lacking vocabulary optimization, our proposed method employs orthogonal space constraints to refine the embedding manifold. This

Table 1: Performance of OCP on OxygenREC with 0.7B and 3.2B parameters. In this paper, 1e denotes 10^8 . OCP consistently improves Top1 hit@k ($k = 1, 2, 3$).

Params	Method	Vocab size	Hit1	Hit2	Hit3
0.7B model	base	5e	23.42%	7.40%	4.57%
	OCP	5e	23.94%	7.58%	4.66%
3.2B model	base	5e	23.50%	7.60%	4.73%
	OCP	5e	23.93%	7.84%	4.90%

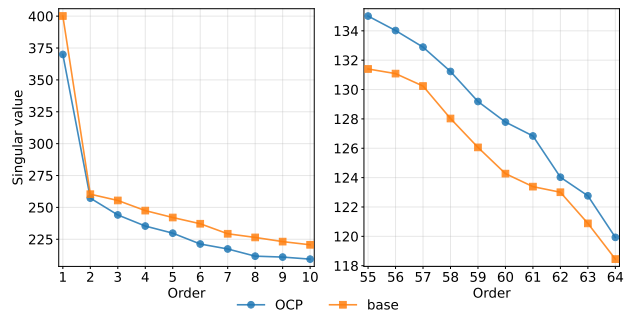


Figure 2: Comparison of singular value distributions. Orders 1–10 and 55–64 represent the top-10 and bottom-10 singular values of the $d = 64$ embedding matrix, respectively.

Table 2: Singular Entropy (SE) results. Higher entropy indicates model's enhanced capacity for sparse representation.

	All data	Bottom 80%	Top 20%
base	0.9725	0.9646	0.9705
OCP	0.9794 (+0.71%)	0.9715 (+0.72%)	0.9787 (+0.85%)

approach effectively enhances the model's capacity for feature generalization while suppressing the overfitting of memorized noise. Consequently, our method achieves a significant gain in predictive performance by maintaining a high-rank representation space.

3.3 Singular Entropy Study

We investigate effect of OCP on geometric stability of Item-ID embeddings using a transformer-based ranking model trained on four months of interaction data from JD.com. The vocabulary size is 1 billion.

To evaluate representation quality, we analyze singular values of the embedding matrix. As shown in Figure 2, OCP reduces overly dominant top singular values while strengthening bottom singular values, indicating a more *isotropic* space and less collapse.

We then conduct stratified analysis on (i) all items, (ii) bottom 80% low-frequency items, and (iii) top 20% high-frequency items. As shown in Table 2, OCP improves SE in all three groups, indicating two effects: it preserves non-zero singular values under column-orthogonal projection and regularizes over-dominant frequent-item directions.

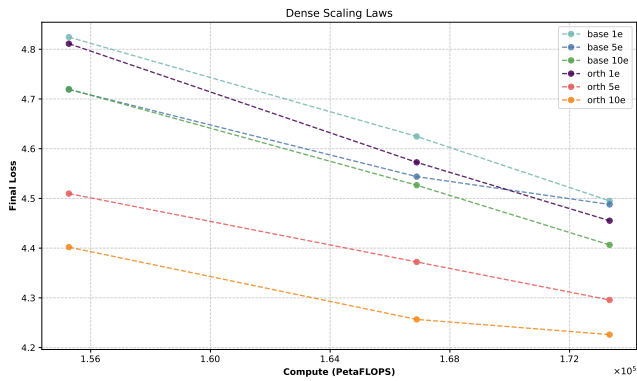


Figure 3: Dense scaling law on OxygenREC with different model sizes. As parameters increase from 0.7B to 1.7B and 3.2B, OCP achieves lower final loss.

3.4 Scaling Law Study with OCP

In this section, we study scaling behavior on both OxygenREC and ranking models to evaluate OCP scalability.

3.4.1 Dense Scaling. As shown in Figure 3, increasing model parameters leads to lower loss and faster convergence under the same training steps. The trend is consistent with standard scaling behavior in recommender training: more dense capacity improves fit quality when optimization remains stable.

3.4.2 Sparse Scaling. As shown for OxygenREC in Figure 4, under the same dense model size, expanding the Item-ID vocabulary results in lower loss. We further run vocabulary ablations on the ranking model by tightening the access threshold (Table 3), which reduces vocabulary size and consistently degrades AUC/GAUC. These results indicate that preserving high-rank Item-ID representations is critical when scaling sparse vocabularies.

3.4.3 What This Validates. Taken together, the dense and sparse scaling results support two complementary conclusions: (1) OCP does not block gains from increasing dense model capacity; (2) OCP makes large sparse vocabularies more useful by preserving representation quality rather than letting extra IDs collapse into noisy low-rank directions.

3.4.4 Discussion on Overhead. OCP introduces a QR-based retraction step for the projection matrix. In our setting, this cost is small compared with the overall training cost dominated by large embedding lookups and transformer interaction layers. Given its consistent gains across retrieval and ranking tasks, OCP provides a favorable trade-off between additional computation and quality improvement in production.

3.5 Online Experiments

We conducted a 5-day online A/B test on JD.com. With OCP, the Item-ID vocabulary scales from 178 million to 1 billion. Combined with a multi-layer self-attention architecture, OCP captures finer long-tail representations and improves key business metrics over production baseline: +12.97% UCXR, +13.07% order volume, and +8.95% GMV.

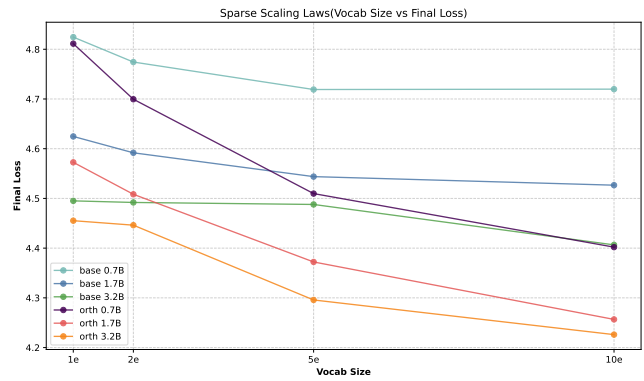


Figure 4: Sparse scaling law on OxygenREC with different vocabulary sizes. As vocabulary increases from 1e (10⁸) to 2e, 5e, and 10e, OCP achieves a lower final loss.

Table 3: Performance under different vocabulary access thresholds. A higher threshold means stricter entry and a smaller vocabulary. Metrics include AUC/GAUC for click (clk) and order (ord).

access threshold	clk AUC	clk GAUC	ord AUC	ord GAUC
15	0.7701	0.6281	0.8158	0.6491
10	0.7738	0.6376	0.8179	0.6519
5	0.7761	0.6404	0.8195	0.6539
3	0.7764	0.6432	0.8199	0.6562

These online gains are directionally consistent with offline findings: better singular-spectrum health and stronger long-tail representation quality translate to measurable business impact.

3.6 Limitations and Future Work

Our current study focuses on a single orthogonality mechanism (QR retraction) and fixed Item-ID vocabulary construction pipelines. Future work includes: (1) comparing alternative manifold optimizers with lower overhead, (2) integrating dynamic vocabulary growth and pruning, and (3) analyzing OCP under stronger distribution shifts (e.g., seasonal and cold-start bursts) with longer online evaluation windows.

4 Conclusion

In this paper, Orthogonal Constrained Projection (OCP) is introduced to improve Item-ID embedding quality under sparse scaling. By constraining the projection matrix on the Stiefel manifold, OCP preserves healthier gradient geometry and mitigates embedding collapse. Experiments on generative retrieval, ranking, and online deployment show that OCP consistently improves convergence and business metrics, and remains robust under both sparse and dense scaling.

References

[1] 2023. Recommender systems with generative retrieval. *Advances in Neural Information Processing Systems* 36 (2023), 10299–10315.

- [2] Jeremy Bernstein. 2025. Modular Manifolds. *Thinking Machines Lab: Connectionism* (2025). doi:10.64434/tml.20250926 <https://thinkingmachines.ai/blog/modular-manifolds/>.
- [3] Paul Covington, Jay Adams, and Emre Sargin. 2016. Deep neural networks for youtube recommendations. In *Proceedings of the 10th ACM conference on recommender systems*. 191–198.
- [4] Huifeng Guo, Ruiming Tang, Yunming Ye, Zhenguo Li, and Xiuqiang He. 2017. DeepFM: a factorization-machine based neural network for CTR prediction. *arXiv preprint arXiv:1703.04247* (2017).
- [5] Xingzhuo Guo, Junwei Pan, Ximei Wang, Baixu Chen, Jie Jiang, and Mingsheng Long. 2024. On the Embedding Collapse when Scaling up Recommendation Models. arXiv:2310.04400 [cs.LG] <https://arxiv.org/abs/2310.04400>
- [6] Xuegang Hao, Ming Zhang, Alex Li, Xiangyu Qian, Zhi Ma, Yanlong Zang, Shijie Yang, Zhongxuan Han, Xiaolong Ma, Jinguang Liu, et al. 2025. OxygenREC: An Instruction-Following Generative Framework for E-commerce Recommendation. *arXiv preprint arXiv:2512.22386* (2025).
- [7] Yupeng Hou, Jiacheng Li, Ashley Shin, Jinsung Jeon, Abhishek Santhanam, Wei Shao, Kaveh Hassani, Ning Yao, and Julian McAuley. 2025. Generating long semantic ids in parallel for recommendation. In *Proceedings of the 31st ACM SIGKDD Conference on Knowledge Discovery and Data Mining V. 2*. 956–966.
- [8] Doyup Lee, Chiheon Kim, Saehoon Kim, Minsu Cho, and Wook-Shin Han. 2022. Autoregressive image generation using residual quantization. In *Proceedings of the IEEE/CVF conference on computer vision and pattern recognition*. 11523–11532.
- [9] Hyunin Lee, Yong Zhang, Hoang Vu Nguyen, Xiaoyi Liu, Namyong Park, Christopher Jung, Rong Jin, Yang Wang, Zhigang Wang, Somayeh Sojoudi, et al. 2025. Cross-attention Secretly Performs Orthogonal Alignment in Recommendation Models. *arXiv preprint arXiv:2510.09435* (2025).
- [10] Jingyuan Liu, Jianlin Su, Xingcheng Yao, Zhejun Jiang, Guokun Lai, Yulun Du, Yidao Qin, Weixin Xu, Enzhe Lu, Junjie Yan, et al. 2025. Muon is scalable for llm training. *arXiv preprint arXiv:2502.16982* (2025).
- [11] Aaron Van Den Oord, Oriol Vinyals, et al. 2017. Neural discrete representation learning. *Advances in neural information processing systems* 30 (2017).
- [12] Shikang Wu, Hui Lu, Jinqiu Jin, Zheng Chai, Shiyong Hong, Junjie Zhang, Shanlei Mu, Kaiyuan Ma, Tianyi Liu, Yuchao Zheng, et al. 2026. MSN: A Memory-based Sparse Activation Scaling Framework for Large-scale Industrial Recommendation. *arXiv preprint arXiv:2602.07526* (2026).
- [13] Lee Xiong, Zhirong Chen, Rahul Mayuranath, Shangran Qiu, Arda Ozdemir, Lu Li, Yang Hu, Dave Li, Jingtao Ren, Howard Cheng, et al. 2026. LLaTTE: Scaling Laws for Multi-Stage Sequence Modeling in Large-Scale Ads Recommendation. *arXiv preprint arXiv:2601.20083* (2026).
- [14] Yi Xu, Chaofan Fan, Jinxin Hu, Yu Zhang, Zeng Xiaoyi, and Jing Zhang. 2025. STORE: Semantic Tokenization, Orthogonal Rotation and Efficient Attention for Scaling Up Ranking Models. *arXiv preprint arXiv:2511.18805* (2025).
- [15] Yi Xu, Moyu Zhang, Chaofan Fan, Jinxin Hu, Xiaochen Li, Yu Zhang, Xiaoyi Zeng, and Jing Zhang. 2025. MMQ-v2: Align, Denoise, and Amplify: Adaptive Behavior Mining for Semantic IDs Learning in Recommendation. *arXiv preprint arXiv:2510.25622* (2025).
- [16] Yi Xu, Moyu Zhang, Chenxuan Li, Zhihao Liao, Haibo Xing, Hao Deng, Jinxin Hu, Yu Zhang, Xiaoyi Zeng, and Jing Zhang. 2025. Mmq: Multimodal mixture-of-quantization tokenization for semantic id generation and user behavioral adaptation. *arXiv preprint arXiv:2508.15281* (2025).
- [17] Junwei Yin, Senjie Kou, Changhao Li, Shuli Wang, Xue Wei, Yinqiu Huang, Yinhua Zhu, Haitao Wang, and Xingxing Wang. 2026. DOS: Dual-Flow Orthogonal Semantic IDs for Recommendation in Meituan. *arXiv preprint arXiv:2602.04460* (2026).
- [18] Guorui Zhou, Xiaoqiang Zhu, Chenru Song, Ying Fan, Han Zhu, Xiao Ma, Yanghui Yan, Junqi Jin, Han Li, and Kun Gai. 2018. Deep interest network for click-through rate prediction. In *Proceedings of the 24th ACM SIGKDD international conference on knowledge discovery & data mining*. 1059–1068.